

# Instantaneous electric energy and electric power dissipation in dispersive media

Wonseok Shin,<sup>1</sup> Aaswath Raman,<sup>2</sup> and Shanhui Fan<sup>1,\*</sup>

<sup>1</sup>Department of Electrical Engineering, Stanford University, Stanford, California 94305, USA

<sup>2</sup>Department of Applied Physics, Stanford University, Stanford, California 94305, USA

\*Corresponding author: shanhui@stanford.edu

Received November 14, 2011; revised December 26, 2011; accepted December 27, 2011;  
posted January 5, 2012 (Doc. ID 158103); published April 24, 2012

We derive the instantaneous densities of electric energy and electric power dissipation in lossless and lossy dispersive media for a time-harmonic electric field. The instantaneous quantities are decomposed into DC and AC components, some of which are shown to be independent of the dispersion of dielectric constants. The AC component of the instantaneous energy density can be used to visualize propagation of electromagnetic waves through complex 3D structures. © 2012 Optical Society of America

OCIS codes: 260.2110, 260.2030, 260.3910.

## 1. INTRODUCTION

Understanding the forms of the densities of energy and power dissipation in dispersive media has been a topic of interest for decades [1–4] and has found renewed interest recently due to the development of metamaterials [5–11]. When electric dispersion is concerned [12], a dispersive medium is characterized by a frequency-dependent dielectric constant  $\varepsilon(\omega) = \varepsilon'(\omega) - i\varepsilon''(\omega)$ . Assuming a time-harmonic electric field ( $E$ -field)  $\mathbf{E}(t) = \mathbf{E}_0 e^{i\omega t}$ , it is well-known that in a lossless dispersive medium, where  $\varepsilon''(\omega) = 0$ , the time average of the electric energy density is [3]

$$\bar{u}_e = \frac{1}{4} \frac{d(\omega \varepsilon(\omega))}{d\omega} |\mathbf{E}_0|^2. \quad (1)$$

The time average of the electric energy density is known also in a *lossy* dispersive medium, where  $\varepsilon''(\omega) > 0$ , provided that the medium is a Lorentz medium, i.e.,  $\varepsilon(\omega)$  described by a Lorentz pole [2,6,8,13]. In addition, the time average of the electric power dissipation density in a lossy dispersive medium is [3]

$$\bar{q}_e = \frac{1}{2} \omega \varepsilon''(\omega) |\mathbf{E}_0|^2, \quad (2)$$

which holds for any lossy dispersive medium including the Lorentz medium.

Most of the previous works on electric energy and power dissipation have focused on the time-averaged quantities [Eq. (1) and Eq. (2)]. The present paper, on the other hand, derives the formulae for *instantaneous* electric energy density and electric power dissipation density. The instantaneous quantities in a dispersive medium were also studied in [7], but their analysis was limited to a dielectric constant described by a single Lorentz pole. In contrast, we derive, for a lossless dispersive medium, a formula for the instantaneous energy density for a generic dielectric constant, provided that the  $E$ -field is harmonic in time.

Because we consider a time-harmonic  $E$ -field, each instantaneous quantity is expressed as the sum of the aforementioned time-averaged quantity and sinusoidal oscillation. We refer to the time average and sinusoidal oscillation as the DC and AC components of the instantaneous quantity, respectively.

Examining Eq. (1), we notice that evaluating  $\bar{u}_e$  at a given frequency requires the values of both  $\varepsilon$  and  $d\varepsilon/d\omega$  at the frequency. In other words, measuring  $\varepsilon$  at the frequency alone is insufficient to determine  $\bar{u}_e$ ; we need additional information on the dispersion of  $\varepsilon$ , which is characterized by  $d\varepsilon/d\omega$  in this case. We refer to quantities such as  $\bar{u}_e$  as being “dispersion-dependent.” Interestingly, in contrast to  $\bar{u}_e$ ,  $\bar{q}_e$  of Eq. (2) requires only the value of  $\varepsilon$  at the frequency and does not require the information on the dispersion of  $\varepsilon$ . We refer to quantities such as  $\bar{q}_e$  as being “dispersion-independent.” One of our objectives in this paper is to show that some DC and AC components of the instantaneous quantities in dispersive media are dispersion-independent.

The paper is organized as follows. In Section 2 we introduce the notations and conventions used in this paper. In Section 3 we provide a derivation of the instantaneous electric energy density in a lossless dispersive medium, which is the main result of this paper. Since instantaneous energy density has rarely been discussed in the literature, for completeness we provide the corresponding formula for a lossy Lorentz medium in Section 4 based on a recent work [13]. In Section 5 we derive the instantaneous electric power dissipation density for the same Lorentz medium and investigate the phase relationship between the oscillations of energy and power dissipation. Finally, in Section 6, we demonstrate that direct visualization of the AC component of the instantaneous electromagnetic (EM) energy density provides new insights in frequency-domain simulations of EM wave propagation compared to the conventional approaches.

## 2. NOTATIONS AND CONVENTIONS

Throughout this paper, bold capital symbols are used for complex vector fields, whereas the corresponding curly capital

symbols indicate their real parts; for example,  $\mathcal{E}(t) = \text{Re}\{\mathbf{E}(t)\} = \text{Re}\{\mathbf{E}_0 e^{i\omega t}\}$  for a time-harmonic  $E$ -field.

In equations, c.c. refers to the complex conjugate of the preceding quantity; for instance,  $\mathcal{E}(t) = \text{Re}\{\mathbf{E}(t)\} = \frac{1}{2}(\mathbf{E}(t) + \text{c.c.})$ .

Finally,  $|\mathbf{E}|^2 = \mathbf{E} \cdot \mathbf{E}^*$  and  $\mathbf{E}^2 = \mathbf{E} \cdot \mathbf{E}$ ; note that  $|\mathbf{E}|^2 \neq \mathbf{E}^2$ .

### 3. INSTANTANEOUS ELECTRIC ENERGY DENSITY IN LOSSLESS DISPERSIVE MEDIA

The time-averaged electric energy density in a lossless dispersive medium is Eq. (1). In this section, we extend the derivation of Eq. (1) to calculate the instantaneous electric energy density. Even though a dispersive medium cannot be lossless for all frequencies due to Kramers–Kronig relations [14], many materials such as dielectrics have negligible loss in some frequency bands, where the analysis in this section applies.

By Poynting's theorem and conservation of energy, the instantaneous electric energy density  $u_e(t)$  in a lossless medium satisfies

$$\frac{\partial u_e}{\partial t} = \mathcal{E} \cdot \frac{\partial \mathcal{D}}{\partial t} = \frac{1}{4} \left( \mathbf{E} \cdot \frac{\partial \mathbf{D}}{\partial t} + \mathbf{E}^* \cdot \frac{\partial \mathbf{D}}{\partial t} \right) + \text{c.c.} \quad (3)$$

We integrate Eq. (3) over time to calculate  $u_e(t)$ . Here, following [3], we consider  $\mathbf{E}(t) = \mathbf{E}_0(t) e^{i\omega t}$  as an approximation to a purely time-harmonic  $E$ -field, where the envelope  $\mathbf{E}_0(t)$  varies much more slowly than  $e^{i\omega t}$ . Because  $\mathbf{E}_0(t) = \frac{1}{\sqrt{2\pi}} \int_{-\infty}^{\infty} \mathbf{E}_{0,\alpha} e^{i\alpha t} d\alpha$ , we have

$$\frac{\partial \mathbf{D}}{\partial t} = \frac{1}{\sqrt{2\pi}} \int_{-\infty}^{\infty} i(\omega + \alpha) \varepsilon(\omega + \alpha) \mathbf{E}_{0,\alpha} e^{i(\omega + \alpha)t} d\alpha. \quad (4)$$

Because of the slowly varying envelope assumption,  $\mathbf{E}_{0,\alpha}$ , and thus the integrand of Eq. (4), is nonzero only for  $\alpha \simeq 0$ . Since  $(\omega + \alpha)\varepsilon(\omega + \alpha) \simeq \omega\varepsilon(\omega) + \frac{d(\omega\varepsilon(\omega))}{d\omega}\alpha$  for  $\alpha \simeq 0$ , Eq. (4) is approximated to

$$\frac{\partial \mathbf{D}}{\partial t} \simeq \left[ i\omega\varepsilon(\omega)\mathbf{E}_0(t) + \frac{d(\omega\varepsilon(\omega))}{d\omega} \frac{\partial \mathbf{E}_0(t)}{\partial t} \right] e^{i\omega t}. \quad (5)$$

From now on, we write  $\varepsilon(\omega)$  as  $\varepsilon$  for simplicity. Substituting Eq. (5) to Eq. (3) gives

$$\begin{aligned} \frac{\partial u_e}{\partial t} = \frac{1}{4} \left[ \left( i\omega\varepsilon\mathbf{E}_0(t)^2 + \frac{d(\omega\varepsilon)}{d\omega} \mathbf{E}_0(t) \cdot \frac{\partial \mathbf{E}_0(t)}{\partial t} \right) e^{i2\omega t} \right. \\ \left. + \left( i\omega\varepsilon|\mathbf{E}_0(t)|^2 + \frac{d(\omega\varepsilon)}{d\omega} \mathbf{E}_0(t)^* \cdot \frac{\partial \mathbf{E}_0(t)}{\partial t} \right) \right] + \text{c.c.} \quad (6) \end{aligned}$$

Because  $\varepsilon^* = \varepsilon$  for a lossless medium, Eq. (6) is further simplified to

$$\begin{aligned} \frac{\partial u_e}{\partial t} = \frac{1}{4} \left[ 2\omega\varepsilon \text{Re}\{i\mathbf{E}_0(t)^2 e^{i2\omega t}\} + \frac{d(\omega\varepsilon)}{d\omega} \text{Re}\left\{ 2\mathbf{E}_0(t) \cdot \frac{\partial \mathbf{E}_0(t)}{\partial t} e^{i2\omega t} \right\} \right. \\ \left. + \frac{d(\omega\varepsilon)}{d\omega} \frac{\partial}{\partial t} |\mathbf{E}_0(t)|^2 \right]. \quad (7) \end{aligned}$$

To express  $\partial u_e / \partial t$  in terms of  $\mathbf{E}(t)$ , we use  $\mathbf{E}_0(t) = \mathbf{E}(t) e^{-i\omega t}$ . Then, Eq. (7) reduces to

$$\frac{\partial u_e}{\partial t} = -\frac{1}{2}\omega^2 \frac{d\varepsilon}{d\omega} \text{Re}\{i\mathbf{E}(t)^2\} + \frac{1}{2} \frac{d(\omega\varepsilon)}{d\omega} \frac{\partial}{\partial t} \mathcal{E}(t)^2. \quad (8)$$

By integrating Eq. (8) over time, we obtain the instantaneous electric energy density

$$u_e(t) = \frac{1}{2} \frac{d(\omega\varepsilon)}{d\omega} \mathcal{E}(t)^2 - \frac{1}{2} \omega^2 \frac{d\varepsilon}{d\omega} \text{Re}\left\{ \int i\mathbf{E}(t)^2 dt \right\} + C, \quad (9)$$

where  $C$  is a constant of integration.

For a purely time-harmonic field  $\mathbf{E}(t) = \mathbf{E}_0 e^{i\omega t}$ , Eq. (9) reduces to

$$\begin{aligned} u_e(t) &= \frac{1}{2} \frac{d(\omega\varepsilon)}{d\omega} \mathcal{E}(t)^2 - \frac{1}{4} \omega \frac{d\varepsilon}{d\omega} \text{Re}\{\mathbf{E}(t)^2\} + C \\ &= \frac{1}{4} \frac{d(\omega\varepsilon)}{d\omega} |\mathbf{E}_0|^2 + \frac{1}{4} \varepsilon \text{Re}\{\mathbf{E}(t)^2\} + C, \quad (10) \end{aligned}$$

where we have utilized an identity

$$\mathcal{W}^2 = \frac{1}{4} (\mathbf{W} + \mathbf{W}^*)^2 = \frac{1}{2} |\mathbf{W}|^2 + \frac{1}{2} \text{Re}\{\mathbf{W}^2\} \quad (11)$$

that holds for any complex vector field  $\mathbf{W}$  and its real part  $\mathcal{W}$ . The comparison of Eq. (10) with the well-known result [Eq. (1)] proves  $C = 0$  because the time average of the second term of Eq. (10) is zero. Therefore, the instantaneous electric energy density for a time-harmonic field is

$$u_e(t) = \bar{u}_e + \tilde{u}_e(t), \quad (12)$$

where the DC component  $\bar{u}_e$  is Eq. (1) and the AC component  $\tilde{u}_e(t)$  is

$$\tilde{u}_e(t) = \frac{1}{4} \varepsilon' \text{Re}\{\mathbf{E}(t)^2\} \quad \text{for} \quad \varepsilon'' = 0. \quad (13)$$

By comparing Eq. (1) and Eq. (13) we notice that the AC component of  $u_e(t)$  is dispersion-independent, whereas the DC component of  $u_e(t)$  is dispersion-dependent. Therefore, in a lossless dispersive medium, if we are interested only in the amplitude and phase of the oscillation of the instantaneous electric energy density, we do not require knowledge of the dispersion of  $\varepsilon$ ; the only information of  $\varepsilon$  needed is the value of  $\varepsilon$  at the frequency of the  $E$ -field.

We also note that the AC component [Eq. (13)] for a lossless medium is either in-phase with  $\text{Re}\{\mathbf{E}(t)^2\}$  for  $\varepsilon' > 0$  or 180° out-of-phase with  $\text{Re}\{\mathbf{E}(t)^2\}$  for  $\varepsilon' < 0$ .

### 4. INSTANTANEOUS ELECTRIC ENERGY DENSITY IN LOSSY DISPERSIVE MEDIA

In general, Poynting's theorem

$$-\oint_S (\mathcal{E} \times \mathcal{H}) \cdot d\mathbf{a} = \int_V \left( \mathcal{E} \cdot \frac{\partial \mathcal{D}}{\partial t} + \mathcal{H} \cdot \frac{\partial \mathcal{B}}{\partial t} \right) dv \quad (14)$$

holds for both lossy and lossless media, with  $-\oint_S (\mathcal{E} \times \mathcal{H}) \cdot d\mathbf{a}$  being the power influx through the surface  $S$  enclosing a volume  $V$ . On the other hand, by considering energy conservation alone, in a lossy medium we expect that

$$-\oint_S (\mathcal{E} \times \mathcal{H}) \cdot d\mathbf{a} = \int_V \left( \frac{\partial u_e}{\partial t} + \frac{\partial u_m}{\partial t} \right) dv + \int_V (q_e + q_m) dv, \quad (15)$$

where  $u_m(t)$  is the instantaneous magnetic energy density;  $q_e(t)$  and  $q_m(t)$  are the instantaneous electric and magnetic power dissipation densities, respectively. Comparing Eq. (14) and Eq. (15), we see that for lossy media it is no longer possible to identify the integrand of the right-hand side of Eq. (14) as the time derivative of the energy density, like we did in Section 3 for lossless media. As a result, Eq. (1) is in general not correct for a lossy dispersive medium [2,6,7,9].

In this and the next sections, we provide derivations of  $u_e(t)$  and  $q_e(t)$  in a lossy dispersive medium. For this purpose, we follow [2,6–8,13] and consider a medium whose dielectric function is described by multiple Lorentz poles:

$$\epsilon(\omega) = \epsilon_\infty \left( 1 + \sum_{i=1}^N \frac{\omega_{p,i}^2}{\omega_{0,i}^2 - \omega^2 + i\omega\Gamma_i} \right). \quad (16)$$

The  $i$ th pole in the dielectric function can be understood as resulting from electrons moving in a harmonic potential characterized by the resonance frequency  $\omega_{0,i}$  while experiencing a damping force with the damping coefficient  $\Gamma_i$ . When an  $E$ -field is applied, the equation of motion for such an electron is

$$m \frac{d^2 r_i}{dt^2} = -m\Gamma_i \frac{dr_i}{dt} - m\omega_{0,i}^2 r_i - e\mathcal{E}, \quad (17)$$

where  $m$ ,  $-e$ ,  $r_i$  are the mass, charge, and the displacement of the electron, respectively. We further assume that the density of such electrons is  $n_i$ . The polarization field  $\mathcal{P}_i$  due to these electrons is then  $\mathcal{P}_i = -n_i e r_i$ , and its dynamics is described by

$$\frac{\partial^2 \mathcal{P}_i}{\partial t^2} + \Gamma_i \frac{\partial \mathcal{P}_i}{\partial t} + \omega_{0,i}^2 \mathcal{P}_i = \omega_{p,i}^2 \epsilon_\infty \mathcal{E}, \quad (18)$$

where  $\omega_{p,i} = \sqrt{n_i e^2 / m \epsilon_\infty}$ . For time-harmonic fields, Eq. (18) dictates

$$-\omega^2 \mathbf{P}_i + i\omega\Gamma_i \mathbf{P}_i + \omega_{0,i}^2 \mathbf{P}_i = \omega_{p,i}^2 \epsilon_\infty \mathbf{E}, \quad (19)$$

from which Eq. (16) recovered.

Now, we define  $\mathcal{V}_i = \partial \mathcal{P}_i / \partial t$  that corresponds to the polarization velocity field [13]. Then Eq. (18) can be written as

$$\frac{\partial \mathcal{V}_i}{\partial t} + \Gamma_i \mathcal{V}_i + \omega_{0,i}^2 \mathcal{P}_i = \epsilon_\infty \omega_{p,i}^2 \mathcal{E}. \quad (20)$$

Using  $\mathcal{D} = \epsilon_\infty \mathcal{E} + \mathcal{P}$  and Eq. (20), we obtain

$$\begin{aligned} \mathcal{E} \cdot \frac{\partial \mathcal{D}}{\partial t} &= \sum_{i=1}^N \frac{1}{\epsilon_\infty \omega_{p,i}^2} \Gamma_i \mathcal{V}_i^2 \\ &+ \frac{\partial}{\partial t} \left[ \frac{1}{2} \epsilon_\infty \mathcal{E}^2 + \sum_{i=1}^N \frac{\omega_{0,i}^2}{2\epsilon_\infty \omega_{p,i}^2} \mathcal{P}_i^2 + \sum_{i=1}^N \frac{1}{2\epsilon_\infty \omega_{p,i}^2} \mathcal{V}_i^2 \right]. \end{aligned} \quad (21)$$

Substituting Eq. (21) in Eq. (14) and equating Eq. (14) to Eq. (15), we have

$$q_e(t) = \sum_{i=1}^N \frac{1}{\epsilon_\infty \omega_{p,i}^2} \Gamma_i \mathcal{V}_i^2, \quad (22)$$

which is the density of the power dissipated by electric damping, and

$$u_e(t) = \frac{1}{2} \epsilon_\infty \mathcal{E}^2 + \sum_{i=1}^N \frac{\omega_{0,i}^2}{2\epsilon_\infty \omega_{p,i}^2} \mathcal{P}_i^2 + \sum_{i=1}^N \frac{1}{2\epsilon_\infty \omega_{p,i}^2} \mathcal{V}_i^2, \quad (23)$$

where the three terms in the right-hand side are the densities of the energy of the  $E$ -field, potential energy of the electrons, and kinetic energy of the electrons. Equations (22) and (23) are consistent with [2,6,7,13]. We note that Eq. (22) and Eq. (23) are valid for any time-varying  $\mathcal{E}(t)$ .

For a time-harmonic  $\mathcal{E}(t)$ , we now reduce Eq. (23) into a formula that is independent of the fields other than  $\mathbf{E}(t)$ . From Eq. (19) we have

$$\mathbf{P}_i(t) = \epsilon_\infty \frac{\omega_{p,i}^2}{\omega_{0,i}^2 - \omega^2 + i\omega\Gamma_i} \mathbf{E}(t), \quad (24)$$

and therefore

$$\mathbf{V}_i(t) = \frac{\partial \mathbf{P}_i(t)}{\partial t} = \epsilon_\infty \frac{i\omega\omega_{p,i}^2}{\omega_{0,i}^2 - \omega^2 + i\omega\Gamma_i} \mathbf{E}(t). \quad (25)$$

We decompose  $\mathcal{E}^2$ ,  $\mathcal{P}_i^2$ , and  $\mathcal{V}_i^2$  in Eq. (23) into DC and AC components by Eq. (11) and use Eq. (24) and Eq. (25) to obtain

$$u_e(t) = \bar{u}_e + \tilde{u}_e(t) \quad (26)$$

with the DC component

$$\bar{u}_e = \frac{1}{4} \epsilon_\infty \left( 1 + \sum_{i=1}^N \frac{\omega_{p,i}^2 (\omega_{0,i}^2 + \omega^2)}{(\omega_{0,i}^2 - \omega^2)^2 + \omega^2 \Gamma_i^2} \right) |\mathbf{E}_0|^2 \quad (27)$$

and the AC component

$$\tilde{u}_e(t) = \frac{1}{4} \epsilon_\infty \operatorname{Re} \left\{ \left( 1 + \sum_{i=1}^N \frac{\omega_{p,i}^2 (\omega_{0,i}^2 - \omega^2)}{(\omega_{0,i}^2 - \omega^2 + i\omega\Gamma_i)^2} \right) \mathbf{E}(t)^2 \right\}. \quad (28)$$

Equations (27) and (28) agree with Eq. (1) and Eq. (13), respectively, when we use the dielectric function of Eq. (16) with  $\Gamma_i = 0$ . We note that Eq. (28) is considerably simplified in cases where the Lorentz medium consists of a single pole, as shown in Appendix A.

For  $u_e(t)$ , both its DC component [Eq. (27)] and AC component [Eq. (28)] depend on the parameters  $\omega_{0,i}$ ,  $\omega_{p,i}$ ,  $\Gamma_i$ , and  $\epsilon_\infty$ . These parameters cannot be determined from the value of the  $\epsilon$  of Eq. (16) at single  $\omega$ . Therefore, both  $\bar{u}_e$  and  $\tilde{u}_e(t)$  for a lossy dispersive medium are dispersion-dependent.

We also note that the AC component [Eq. (28)] for a lossy medium is in general out-of-phase with  $\operatorname{Re}\{\mathbf{E}(t)^2\}$ . This is due to the phase delay in  $\mathcal{P}_i(t)$  with respect to  $\mathcal{E}(t)$ ; in a damped harmonic oscillator, the displacement typically lags behind the driving force [15,16]. Because  $\mathcal{P}_i(t)$ , and thus  $\mathcal{V}_i(t)$ , is out-of-phase with  $\mathcal{E}(t)$  in general, we see from Eq. (23) that  $u_e(t)$  and  $\mathcal{E}(t)^2$ , or their AC components  $\tilde{u}_e(t)$  and  $\frac{1}{2} \operatorname{Re}\{\mathbf{E}(t)^2\}$ , do not oscillate in-phase for a time-harmonic  $\mathcal{E}(t)$ .

We end this section by noting that the instantaneous energy density  $u_e(t)$  is always positive, as can be seen from Eq. (23). From Eq. (26) we therefore have  $\tilde{u}_e(t) \geq -\bar{u}_e$ . Since the AC component  $\tilde{u}_e(t)$  oscillates sinusoidally, this further implies that

$$-\bar{u}_e \leq \tilde{u}_e(t) \leq \bar{u}_e. \quad (29)$$

In other words, the amplitude of the AC component of the instantaneous energy density cannot exceed the time-averaged energy density. Also,

$$0 \leq u_e(t) \leq 2\bar{u}_e, \quad (30)$$

so the instantaneous energy density, which is always positive, does not exceed twice the time-averaged energy density.

## 5. INSTANTANEOUS ELECTRIC POWER DISSIPATION DENSITY IN LOSSY DISPERSIVE MEDIA

For a time-harmonic  $E$ -field, we decompose  $\mathcal{V}_i^2$  in Eq. (22) into DC and AC components by Eq. (11) and use Eq. (25) to obtain

$$q_e(t) = \bar{q}_e + \tilde{q}_e(t) \quad (31)$$

with the DC component

$$\bar{q}_e = \frac{1}{2} \varepsilon_\infty \sum_{i=1}^N \frac{\omega_{p,i}^2 \omega^2 \Gamma_i}{(\omega_{0,i}^2 - \omega^2)^2 + \omega^2 \Gamma_i^2} |\mathbf{E}_0|^2 \quad (32)$$

and the AC component

$$\tilde{q}_e(t) = -\frac{1}{2} \varepsilon_\infty \operatorname{Re} \left\{ \sum_{i=1}^N \frac{\omega_{p,i}^2 \omega^2 \Gamma_i}{(\omega_{0,i}^2 - \omega^2 + i\omega \Gamma_i)^2} \mathbf{E}(t)^2 \right\}. \quad (33)$$

Because Eqs. (32) and (33) depend on the parameters  $\omega_{0,i}$ ,  $\omega_{p,i}$ ,  $\Gamma_i$ , and  $\varepsilon_\infty$  that cannot be determined by the value of the  $\varepsilon$  of Eq. (16) at single  $\omega$ , it would seem that both the DC and AC components of  $q_e(t)$  are dispersion-dependent. However, it turns out that Eq. (33) reduces to Eq. (2), so the DC component of  $q_e(t)$  is dispersion-independent. On the other hand, the AC component of  $q_e(t)$  is dispersion-dependent, because it satisfies

$$\frac{\tilde{q}_e(t + \pi/4\omega)}{2\omega} = \tilde{u}_e(t) - \frac{1}{4} \operatorname{Re}\{\varepsilon \mathbf{E}(t)^2\}, \quad (34)$$

which can be proved by direct substitution of Eqs. (16), (28), and (33). The first term of the right-hand side of Eq. (34) is dispersion-dependent as shown at the end of Section 4, whereas the second term is not. Hence, the left-hand side of Eq. (34) should be dispersion-dependent.

Table 1 summarizes the dispersion dependencies of the DC and AC components of the instantaneous quantities examined so far.

We now investigate the relationship between the oscillation phases of the instantaneous electric energy density, power dissipation density, and electric field. We consider silver as an example of a lossy material. The parameters  $\omega_{0,i}$ ,  $\omega_{p,i}$ ,  $\Gamma_i$ , and  $\varepsilon_\infty$  describing the  $\varepsilon(\omega)$  of silver are taken from [17].

**Table 1. Dispersion Dependencies of the DC and AC Components of the Instantaneous Electric Energy Density  $u_e(t)$  and Instantaneous Electric Power Dissipation Density  $q_e(t)$  in Lossless and Lossy Dispersive Media<sup>a</sup>**

	Lossless	Lossy	
	$u_e$	$u_e$	$q_e$
DC	<i>D</i>	<i>D</i>	<i>I</i>
AC	<i>I</i>	<i>D</i>	<i>D</i>

<sup>a</sup>*D* indicates dispersion-dependent, and *I* indicates dispersion-independent.

Using these parameters, we evaluate  $\tilde{u}_e(t)$  and  $\tilde{q}_e(t)$  in silver for two vacuum wavelengths  $\lambda_0 = 620$  nm and  $\lambda_0 = 1550$  nm, for both of which  $\varepsilon''_{\text{Ag}}/\varepsilon'_{\text{Ag}} \simeq -0.08$ .

Figure 1 displays  $\tilde{u}_e(t)$  and  $\tilde{q}_e(t)$  for the two vacuum wavelengths;  $\operatorname{Re}\{\mathbf{E}(t)^2\}$  is also plotted for comparison. We first note that  $\tilde{u}_e(t)$  is nearly 180° out-of-phase with  $\operatorname{Re}\{\mathbf{E}(t)^2\}$ . This is because  $|\varepsilon''_{\text{Ag}}/\varepsilon'_{\text{Ag}}| \ll 1$  and thus silver can be treated as nearly lossless for both the wavelengths; see the comment at the end of Section 3.

We also compare the phases of  $\tilde{u}_e(t)$  and  $\tilde{q}_e(t)$ . Because

$$\tilde{u}_e(t) \simeq (\text{Equation (13)}) \simeq \frac{1}{4} \operatorname{Re}\{\varepsilon \mathbf{E}(t)^2\} \quad \text{for } |\varepsilon''/\varepsilon'| \ll 1, \quad (35)$$

the magnitude of  $\tilde{u}_e(t) - \frac{1}{4} \operatorname{Re}\{\varepsilon \mathbf{E}(t)^2\}$  is close to zero. However, Eq. (35) does not impose any restriction on the phase of  $\tilde{u}_e(t) - \frac{1}{4} \operatorname{Re}\{\varepsilon \mathbf{E}(t)^2\}$ . As a result, the phase of  $\tilde{q}_e(t)$  in Eq. (34) can have a range of values, as demonstrated in Figs. 1(a) and 1(b). In particular, Fig. 1(a) implies that the instantaneous densities of electric energy and electric power dissipation are not necessarily maximized at the same time, even if the medium is nearly lossless. We also note that the phases of  $\tilde{q}_e(t)$  in Figs. 1(a) and 1(b) are quite different regardless of the nearly identical loss tangents  $\varepsilon''_{\text{Ag}}/\varepsilon'_{\text{Ag}} \simeq -0.08$  for the two wavelengths used.

## 6. VISUALIZATION OF THE AC COMPONENT OF THE INSTANTANEOUS EM ENERGY DENSITY CARRIED BY EM WAVES

In this section, we demonstrate that visualizing the AC component of the instantaneous EM energy density in numerical simulations provides new insights into photonic device physics.

In frequency-domain EM simulations, it is conventional to visualize simulation results by plotting a single coordinate component of the  $E$ - or  $H$ -field (e.g.,  $E_x$  in the Cartesian coordinate system,  $H_\varphi$  in the spherical coordinate system). However, this method describes the propagation of EM waves correctly only when the field is polarized dominantly in one direction, which is in general not true for waves propagating through 3D structures.

For example, consider EM wave propagation through a metallic slot waveguide bend [18] illustrated in Fig. 2. Such a slot waveguide structure is important in integrated nanophotonics since it provides broadband nanoscale guidance of EM waves [19]. Our numerical simulation of a metallic slot waveguide



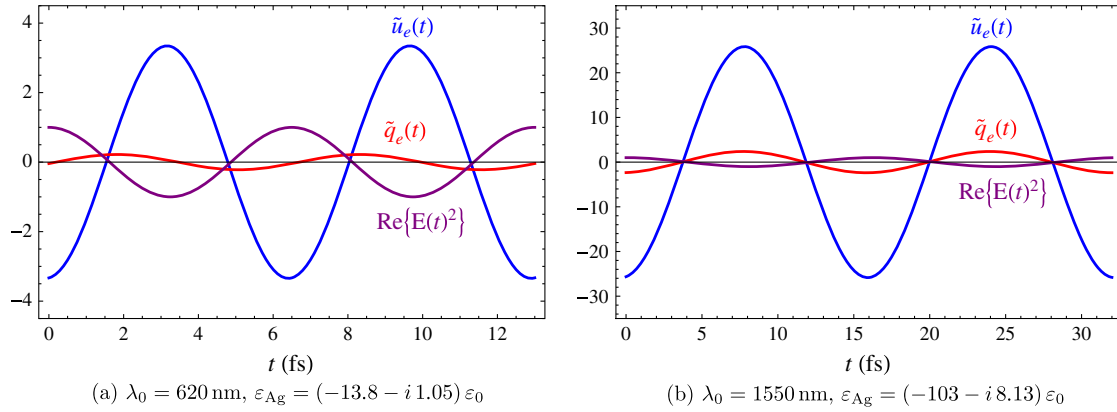


Fig. 1. (Color online) Plots of  $\tilde{u}_e(t)$ ,  $\tilde{q}_e(t)$  and  $\text{Re}\{\mathbf{E}(t)^2\}$  for time-harmonic electric fields  $\mathbf{E}(t) = \hat{x} E_0 e^{i\omega t}$  in silver (Ag). The quantities are plotted for two vacuum wavelengths: (a)  $\lambda_0 = 620$  nm and (b)  $\lambda_0 = 1550$  nm. Note that  $\tilde{u}_e(t)$  is nearly  $180^\circ$  out-of-phase with  $\text{Re}\{\mathbf{E}(t)^2\}$  for both cases. Also notice that  $\tilde{q}_e(t)$  is out-of-phase with  $\tilde{u}_e(t)$  in (a) whereas it is nearly in-phase with  $\tilde{u}_e(t)$  in (b). The units of  $\tilde{u}_e(t)$ ,  $\tilde{q}_e(t)$ , and  $\text{Re}\{\mathbf{E}(t)^2\}$  in the vertical axes are  $\epsilon_0 E_0^2$ ,  $\omega \epsilon_0 E_0^2$ , and  $E_0^2$ , respectively.

bend described in Fig. 2 reveals that the transmission is about 80% at a vacuum wavelength  $\lambda_0 = 1550$  nm. The rest of the incident power divides into the two leakage channels indicated in Fig. 2: about 10% of the incident power couples into a surface plasmon mode bound to the metal film, and another 10% radiates into the background dielectric.

Now, we consider the visualization of the EM wave that best illustrates the underlying physics. One could plot a single Cartesian component of the EM field. In this case, because  $H_y$  is the only EM field component that is dominant inside the slot waveguide both before and after the bend, it is natural to plot  $H_y$  over all space. However, as shown in Fig. 3(a), while the plot of  $H_y$  indeed describes light going around the bend, it displays neither the energy leaking into the surface mode nor the

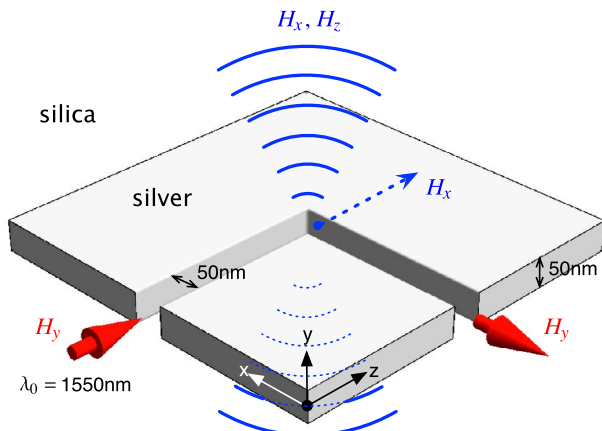


Fig. 2. (Color online) Metallic slot waveguide bend composed of two silver (Ag) films immersed in silica ( $\text{SiO}_2$ ). The two red arrows indicate the directions of the energy flow inside the slot region before and after the bend. The dashed blue arrow indicates the energy leakage into a mode bound to the metal film. The blue arcs indicate the radiation into the background silica. The dominant  $H$ -field component is shown for each energy flow channel. Note that the leakage channels have the dominant  $H$ -field polarized in different directions than the slot waveguide channel. The vacuum wavelength and relevant dimensions of the structure are indicated in the figure. At the specified vacuum wavelength, the dielectric constants of Ag [20] and  $\text{SiO}_2$  [21] are  $\epsilon_{\text{Ag}} = (-129 - i 3.28)\epsilon_0$  and  $\epsilon_{\text{SiO}_2} = 2.085\epsilon_0$ , respectively. The magnetic permeabilities of both materials are  $\mu_0$ .

spherical wavefronts that are characteristic of the radiation into the background dielectric.

Alternatively, one may plot the time-averaged EM energy density  $\tilde{u}$  as in Fig. 3(b). The time-averaged EM energy density is a scalar quantity that contains contributions from all components of the  $E$ - and  $H$ -fields, so it can show the distribution of energy in space properly without being sensitive to variation in the dominant polarization direction. However, since the time-averaged EM energy density does not contain any phase information, it cannot describe wave propagation.

To overcome the limitations of plotting a single Cartesian component of the EM field or the time-averaged EM energy density, we can plot the AC component  $\tilde{u} = \tilde{u}_e + \tilde{u}_m$  of the instantaneous EM energy density. The AC component of the instantaneous EM energy density has the merits of both quantities discussed above: it retains phase information like a single Cartesian component of the EM field, and it is insensitive to variation in the dominant polarization direction of the EM field like the time-averaged EM energy density. Therefore,  $\tilde{u}$  is indeed an appropriate quantity to plot to visualize EM wave propagation through arbitrary 3D routes.

Figure 3(c) visualizes  $\tilde{u}$  for the same solution of the frequency-domain Maxwell's equations used in Fig. 3(a) and 3(b). The resulting plot successfully shows high transmission through the bend, and it also correctly describes the energy coupled to the surface plasmon mode and the spherical wavefronts of the radiation. Moreover, the plot clearly shows the phase variation of the field. Note, however, that the spatial frequency of  $\tilde{u}$  in Fig. 3(c) is twice as fast as that of  $H_y$  in Fig. 3(a) because  $\tilde{u}$  contains  $\mathbf{E}^2$  and  $\mathbf{H}^2$ .

One could visualize  $\text{Re}\{\mathbf{E}^2\}$  to achieve the same advantages that the plot of  $\tilde{u}$  has. However, we note that  $\tilde{u}$  has a direct physical significance, and it also includes the contributions from both the electric and magnetic fields.

In calculating  $\tilde{u} = \tilde{u}_e + \tilde{u}_m$  for Fig. 3(c), we use Eq. (13) for  $\tilde{u}_e$  and  $\frac{1}{4}\mu_0 \text{Re}\{\mathbf{H}^2\}$  for  $\tilde{u}_m$  at each spatial point. Even though silver is lossy, the loss is very small at the wavelength used; linear interpolation of the experimentally measured data tabulated in [20] gives  $\epsilon_{\text{Ag}} = (-129 - i 3.28)\epsilon_0$  as the dielectric constant of silver at  $\lambda_0 = 1550$  nm, so  $|\epsilon''_{\text{Ag}}/\epsilon'_{\text{Ag}}| \simeq 0.0254 \ll 1$ . Therefore, silver is nearly lossless to the infrared wave used in the numerical simulation, so the use of Eq. (13) is valid as

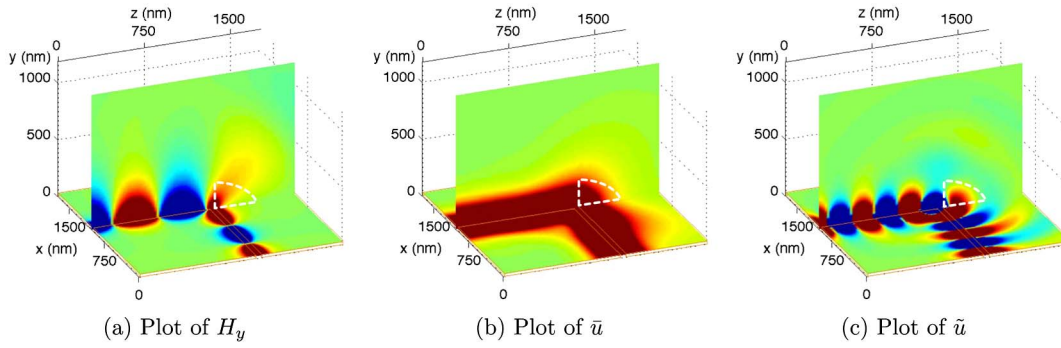


Fig. 3. (Color online) Visualization of wave propagation through the metallic slot waveguide bend. The fields here are obtained by solving the frequency-domain Maxwell's equations using the finite-difference frequency-domain method. The quantities (a)  $H_y$ , (b) time-averaged energy density  $\bar{u} = \bar{u}_e + \bar{u}_m$ , and (c) AC component of instantaneous energy density  $\tilde{u} = \tilde{u}_e + \tilde{u}_m$  of the solution of the frequency-domain Maxwell's equations are plotted on two planes: a horizontal  $y = (\text{const.})$  plane on top of the metal film and a vertical  $x = (\text{const.})$  plane containing the central axis of the input port. Red, green, and blue indicate positive, zero, and negative, respectively. The area enclosed by the white dashed line in each figure is where the coupling of the EM energy into the surface plasmon mode is supposed to be observed. Note that (a) fails to capture such a coupling; (b) captures the coupling but loses the phase information; (c) displays both the coupling and phase information properly. Also notice the weak but discernible pattern of spherical wavefronts in the vertical plane in (c). The thin orange lines around the  $y = 0$  plane outline the two metal pieces.

shown in Eq. (35). In cases where substantially lossy materials are used, we can still calculate  $\tilde{u}_e$  using Eq. (28) with fitting parameters tabulated in the literature such as [17] or using a simple method introduced in Appendix A that requires a single fitting parameter  $\epsilon_\infty$  when  $\omega$  is close to a resonance frequency of  $\epsilon(\omega)$ .

## 7. CONCLUSION

We have derived an expression for the instantaneous electric energy density in lossless dispersive media for a time-harmonic electric field. For lossy dispersive media described by Lorentz poles, we have derived an expression for the instantaneous electric power dissipation density as well as the instantaneous electric energy density.

Each instantaneous quantity is decomposed into DC and AC components. Interestingly, some of the DC and AC components do not depend on the dispersion of dielectric constants. The AC component of the instantaneous EM energy density exhibits wavelike oscillation and contains contributions from all polarization components of the EM field. Plotting such a quantity therefore provides a convenient and informative way to visualize energy transport in complex EM structures and future integrated nanophotonic devices.

## APPENDIX A: SIMPLE METHOD TO CALCULATE THE AC COMPONENTS OF $u_e(t)$ AND $q_e(t)$ FOR LOSSY MEDIA DESCRIBED BY A SINGLE LORENTZ POLE

In this section, we provide a simple method to calculate the AC components of the electric energy density and electric power dissipation density in a lossy medium described by a dielectric function with a single Lorentz pole:

$$\epsilon(\omega) = \epsilon_\infty \left( 1 + \frac{\omega_p^2}{\omega_0^2 - \omega^2 + i\omega\Gamma} \right). \quad (\text{A1})$$

The method involves only one fitting parameter  $\epsilon_\infty$ .

For a medium described by the dielectric function [Eq. (A1)], Eq. (28) reduces to

$$\tilde{u}_e(t) = \frac{1}{4} \text{Re} \left\{ \epsilon_\infty \left( 1 + \frac{\omega_p^2(\omega_0^2 - \omega^2)}{(\omega_0^2 - \omega^2 + i\omega\Gamma)^2} \right) \mathbf{E}(t)^2 \right\}. \quad (\text{A2})$$

The four parameters  $\omega_0$ ,  $\omega_p$ ,  $\Gamma$ , and  $\epsilon_\infty$  needed to calculate Eq. (A2) are typically obtained by fitting experimentally measured  $\epsilon(\omega)$  around  $\omega = \omega_0$  to Eq. (A1).

We seek to simplify Eq. (A2) into a form that involves only the value of  $\epsilon$  at a given  $\omega$  and  $\epsilon_\infty$ . Using the electric susceptibility  $\chi_e(\omega) = \omega_p^2/(\omega_0^2 - \omega^2 + i\omega\Gamma)$ , we rewrite the factor multiplied to  $\mathbf{E}(t)^2$  within the curly braces in Eq. (A2) as

$$\epsilon_\infty \left( 1 + \frac{\omega_p^2(\omega_0^2 - \omega^2)}{(\omega_0^2 - \omega^2 + i\omega\Gamma)^2} \right) = \epsilon_\infty \left( 1 + \chi_e(\omega)^2 \text{Re} \left\{ \frac{1}{\chi_e(\omega)} \right\} \right). \quad (\text{A3})$$

Because  $\chi_e(\omega) = \epsilon(\omega)/\epsilon_\infty - 1$ , Eq. (A3) is also written as

$$\epsilon_\infty \left( 1 + \frac{\omega_p^2(\omega_0^2 - \omega^2)}{(\omega_0^2 - \omega^2 + i\omega\Gamma)^2} \right) = \epsilon_\infty + (\epsilon(\omega) - \epsilon_\infty)^2 \text{Re} \left\{ \frac{1}{\epsilon(\omega) - \epsilon_\infty} \right\}. \quad (\text{A4})$$

By substituting Eq. (A4) in Eq. (A2), we reach

$$\tilde{u}_e(t) = \frac{1}{4} \epsilon_\infty \text{Re} \{ \mathbf{E}(t)^2 \} + \frac{1}{4} \text{Re} \left\{ \frac{1}{\epsilon(\omega) - \epsilon_\infty} \right\} \text{Re} \{ (\epsilon(\omega) - \epsilon_\infty)^2 \mathbf{E}(t)^2 \}. \quad (\text{A5})$$

Equation (A5) allows us to calculate  $\tilde{u}_e(t)$  using a single fitting parameter  $\epsilon_\infty$ ; the other parameter  $\epsilon(\omega)$  in Eq. (A5) is an experimentally measured quantity found in references such as [20,21].

We also obtain a simplified formula for  $\tilde{q}_e(t)$  by substituting Eq. (A5) into Eq. (34):

$$\tilde{q}_e(t) = -\frac{1}{2} \omega \text{Im} \{ (\epsilon(\omega) - \epsilon_\infty) \mathbf{E}(t)^2 \} + \frac{1}{2} \omega \text{Re} \left\{ \frac{1}{\epsilon(\omega) - \epsilon_\infty} \right\} \text{Im} \{ (\epsilon(\omega) - \epsilon_\infty)^2 \mathbf{E}(t)^2 \}. \quad (\text{A6})$$

## ACKNOWLEDGMENTS

We thank Sung Hee Park and Dr. Hyungjin Ma for helpful discussions and comments. This work was supported by the National Science Foundation (Grant No. DMS 09-68809), the MARCO Interconnect Focus Center, and the AFOSR MURI program (Grant No. FA9550-09-1-0704). Wonseok Shin also acknowledges the support of Samsung Scholarship Foundation.

## REFERENCES AND NOTE

1. L. Brillouin, *Wave Propagation and Group Velocity* (Academic, 1960).
2. R. Loudon, "The propagation of electromagnetic energy through an absorbing dielectric," *J. Phys. A: Gen. Phys.* **3**, 233–245 (1970).
3. L. D. Landau and E. M. Lifshitz, *Electrodynamics of Continuous Media* (Butterworth-Heinemann, 1984), 2nd ed. Section 80.
4. V. Polevoi, "Maximum energy extractable from an electromagnetic field," *Radiophys. Quantum Electron.* **33**, 603–609 (1990).
5. R. W. Ziolkowski, "Superluminal transmission of information through an electromagnetic metamaterial," *Phys. Rev. E* **63**, 046604 (2001).
6. R. Ruppin, "Electromagnetic energy density in a dispersive and absorptive material," *Phys. Lett. A* **299**, 309–312 (2002).
7. T. Cui and J. Kong, "Time-domain electromagnetic energy in a frequency-dispersive left-handed medium," *Phys. Rev. B* **70**, 205106 (2004).
8. S. Tretyakov, "Electromagnetic field energy density in artificial microwave materials with strong dispersion and loss," *Phys. Lett. A* **343**, 231–237 (2005).
9. P.-G. Luan, "Power loss and electromagnetic energy density in a dispersive metamaterial medium," *Phys. Rev. E* **80**, 046601 (2009).
10. K. Webb and Shivanand, "Electromagnetic field energy in dispersive materials," *J. Opt. Soc. Am. B* **27**, 1215–1220 (2010).
11. F. D. Nunes, T. C. Vasconcelos, M. Bezerra, and J. Weiner, "Electromagnetic energy density in dispersive and dissipative media," *J. Opt. Soc. Am. B* **28**, 1544–1552 (2011).
12. The derivation given in this paper for electrically dispersive media can be easily extended to magnetically dispersive media, which is described by a frequency-dependent magnetic permeability  $\mu(\omega) = \mu'(\omega) - i\mu''(\omega)$ .
13. A. Raman and S. Fan, "Photonic band structure of dispersive metamaterials formulated as a Hermitian eigenvalue problem," *Phys. Rev. Lett.* 087401 (2010).
14. J. D. Jackson, *Classical Electrodynamics* (Wiley, 1999), 3rd ed. Section 7.10.
15. A. Sommerfeld, *Mechanics* (Academic, 1956). Section III.19.
16. J. B. Marion and S. T. Thornton, *Classical Dynamics of Particles and Systems* (Saunders College, 1995), 4th ed. Section 3.6.
17. A. D. Rakić, A. B. Djurišić, J. M. Elazar, and M. L. Majewski, "Optical properties of metallic films for vertical-cavity optoelectronic devices," *Appl. Opt.* **37**, 5271–5283 (1998).
18. W. Cai, W. Shin, S. Fan, and M. L. Brongersma, "Elements for plasmonic nanocircuits with three-dimensional slot waveguides," *Adv. Mat.* **22**, 5120–5124 (2010).
19. G. Veronis and S. Fan, "Modes of subwavelength plasmonic slot waveguides," *J. Lightwave Technol.* **25**, 2511–2521 (2007).
20. P. B. Johnson and R. W. Christy, "Optical constants of the noble metals," *Phys. Rev. B* **6**, 4370–4379 (1972).
21. E. D. Palik, ed., *Handbook of Optical Constants of Solids* (Academic, 1985).